Megastructure Observability within TESS Light Curves

Piper Stacey[1, 3], Howard Isaacson[1], Steve Croft[1, 2]
Ann Marie Cody[2], Doug Caldwell[2], Brian Powell[2], Marvin Morgan[2, 4]
[1] Breakthrough Listen's Berkeley SETI Research Center, [2] SETI Institute, [3] Dartmouth College, [4] University of Pennsylvania

Table of Contents:

Introduction:

From E.T. to Yoda to Superman from Krypton, as humans, we have many ideas of what extraterrestrial life could look like. However, even with the life forms themselves so elusive, there are other ways that scientists can search for extraterrestrial intelligence. For E.T., this might mean looking for the unnatural lights on his UFO while for Superman and Yoda this could mean looking for artificial heat signatures from their heat vision and lightsaber, respectively. However, another way to search for all three of these advanced aliens would be to search for their spaceships. If we find their technology—their ships—we can find proof of the intelligent life that owns and controls the ships.

In our search for extraterrestrial intelligence, we can now look for artificial photometric signs using the Transiting Exoplanet Survey Satellite (TESS). Since 2018, TESS has surveyed millions of stars in the pursuit of exoplanet transits which occur whenever a planet occludes its host star. But, planets aren't the only objects that can block light from a star. Dust and even other stars are known to change the apparent flux output from a star, at least from our perspective on Earth. But, what about artificial objects? The discovery of an artificial alien megastructure would surely be proof that humans weren't alone as the only intelligent life in the universe. This summer, as an intern for Breakthrough Listen's Berkeley SETI

Research Center, I was tasked with helping search for possible alien megastructures within TESS data. Throughout this summer, I have attempted to help answer these questions:

1. Are artificial megastructures observable within TESS data and to what degree?
2. Are there any artificial megastructures within TESS data?

Megastructure Modeling with EightBitTransit

The first step to answering whether extraterrestrial intelligence (ETI) megastructures are observable using TESS was to model what a megastructure transit would look like. I did this using EightBitTransit, a code developed by Sandford and Kipping 2018. EightBitTransit allows a user to model any shape using a black and white silhouette of their desired object. The program reads grey pixels as varying degrees of opaque where black pixels fully block out the light from the star. Using this program, I first modeled my name:

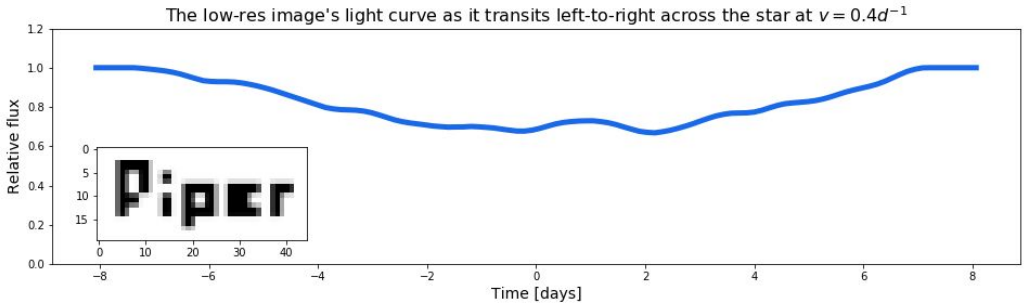

Figure 1: The resulting transit light curve created by the word "Piper" transiting in front of its host star. Modeled using EightBitTransit.

Designing Megastructures Shapes and Patterns:

However, despite how cool it was to prove that EightBitTransit could model anything, I realized that it was quite unlikely that an alien species would choose to write my name as a megastructure that would transit their host star (and at the size of ~20 Jupiters, I figured this was even less likely). So, the next thing to do was to think of reasonable megastructure shapes. First, I asked the question: why would ETI build a megastructure in the first place? Arnold 2005 inspired two reasons why I believe ETI might build an artificial megastructure:

1. For practical use:
    a. The artificial shape would likely be similar to a natural shape to increase familiarity and functionality
        i. Scientific Research (similar to the International Space Station)
        ii. Energy Collection (solar)
        iii. Political Dominance (similar to the space race)
2. For signaling, either:
    a. The megastructure shape allowed the artificial object to be highly observable as something different than a natural planet
    b. The pattern in which megastructures transit is unnatural yet period, suggesting an artificial cause

Examples:

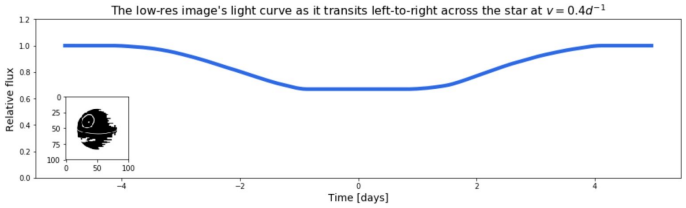

Figure 2: The Death Star from Star Wars transiting in front of its host star as an example of a practical megastructure built similar to a natural shape (moon shaped).

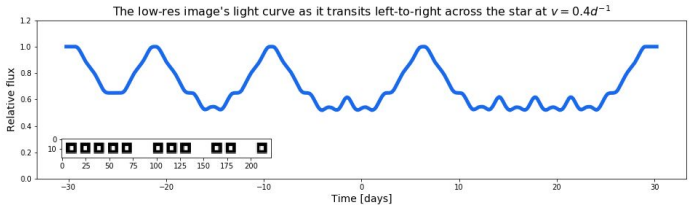

Figure 3: A prime number formation of square panel objects transiting in front of their host star to demonstrate the observability of artificial signaling through megastructure orbital sequence.

Of course, for every odd light curve found to date, there are a host of natural explanations. From young stars with proto-planetary discs to starspots to (rare) interstellar medium, stars can dim with completely reasonable explanations every day—and they do. Therefore, my task was to brainstorm possible megastructure shapes that would create distinguishable transits from the light curves created by natural phenomena. I used the website pixilart.com to make most of my silhouette shapes that I fed into EightBitTransit's modeling algorithm.

Figure 4: Example artificial object silhouettes created with pixilart.com

After creating an assortment of artificial objects, the next step was to inject the EightBitTransit models with standard TESS noise. The purpose of this was to see how observable an object was from a same-sized planet with a noisy light curve.

TESS Noise and Observability:

In order to inject standard TESS noise, I measured the normal (out-of-transit) standard deviation of real TESS data across different magnitudes. I then fit these standard deviations to a line of best fit and used this to simulate standard Gaussian noise for stars of any magnitude. I then double-checked my work with the TESS website and confirmed that my simulated noise was as similar as possible to the values they give.

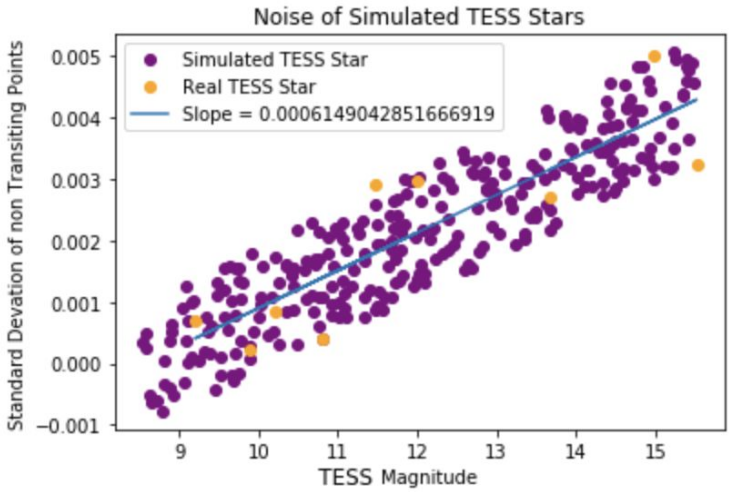

Figure 5: As a star becomes dimmer, the standard deviation of the out-of-transit points increases in a linear fashion. The simulated stars were generated with a non-Gaussian method.

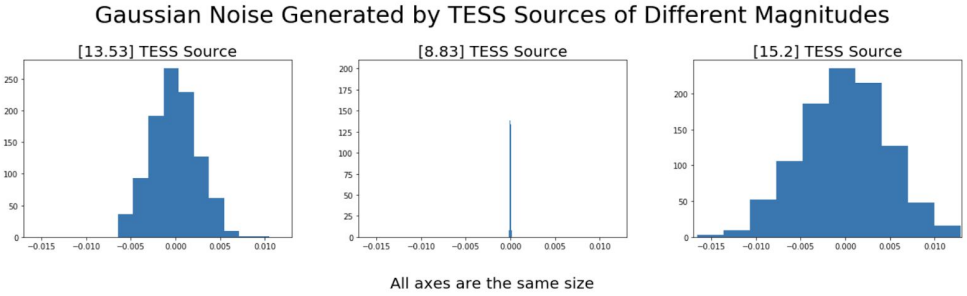

Figure 6: Gaussian noise for an 8.83, a 13.53, and a 15.2 magnitude star. The Gaussian distribution is clearly much wider for dimmer stars.

Now with the ability to model the transit of any object in front of its host star and the ability to simulate the expected TESS noise of any star, I could determine how observable each megastructure object was. To do this, I injected the simulated TESS noise into the light curves of both an artificial object and a same-sized planetary object. Then, I subtracted the planetary object's light curve from the artificial object's light curve (planetary - artificial).

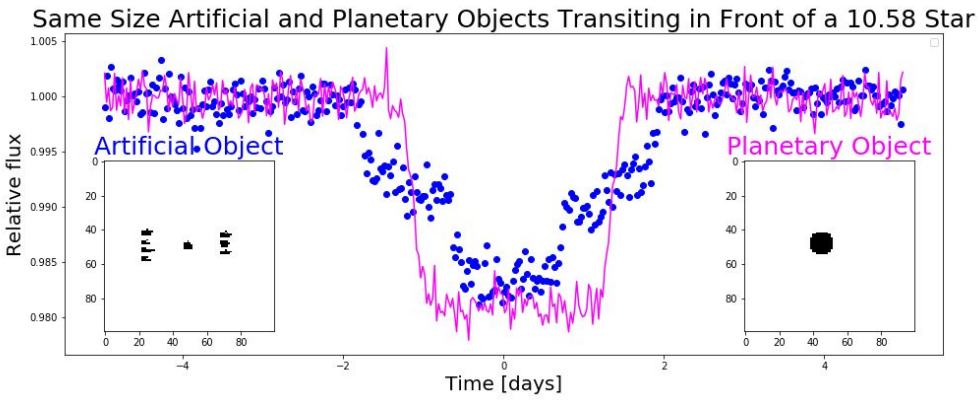

Figure 7: The transit light curve created by the artificial object "Pi Ships" which is the first three digits of pi: 3.14. Also shown is the transit light curve created by a planet of the same size (same total number of pixels) as the artificial object.

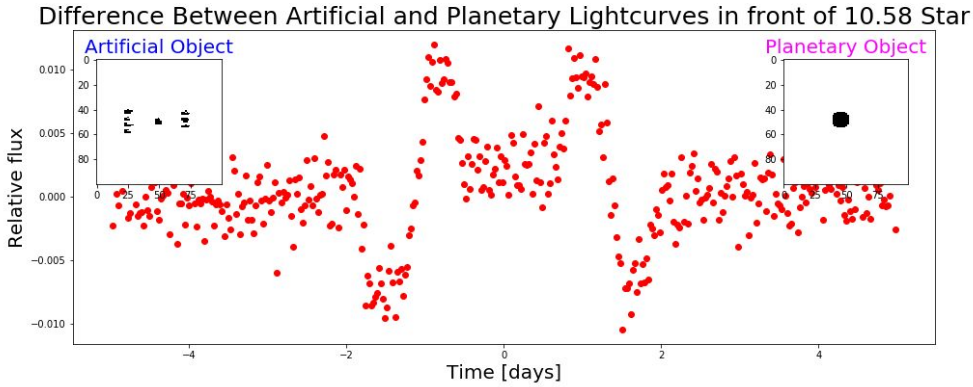

Figure 8:
The residuals (artificial - planetary) of the transit light curve created by the artificial object and the transit light curve created by the planetary object.

Next, I calculated the in-transit RMS residuals as well as the out-of-transit RMS residuals. Using these two measurements, I created an observability index:

$$\text{Observability} = \frac{\textit{[RMS of Residuals of In-Transit Points]}}{\textit{[RMS of Residuals of Out-of-Transit Points]}}$$

The idea with this observability index is that you're effectively creating a ratio of the RMS of the in-transit residuals as they relate to the RMS of the out-of-transit residuals. As a limit to observability, we decided that any object with an observability index of above three is almost certainly observable within TESS light curves. We choose O = 3 to be our threshold because it parallels σ = 3, effectively giving us 99% certainty that the objects with an observability index of three or higher for a particular magnitude of star will be observable as something different than a natural planet.

Non-Circularity and Observability Across Different Magnitudes:

Next, we wanted to characterize non-circularity since that was the main reason for a difference in transit shape between artificial and planetary objects. To measure non-circularity, for each artificial object, we created a same-sized planet. This meant that the planetary object would always have exactly the same number of pixels as the artificial object, ensuring a transit of equal depth. After knowing the area of the corresponding planet, we could determine which parts of the artificial object protruded or were cut out of the area of the matching planet. We measured up the number of the pixels and then used them to create a percentage index of non-circularity:

$$\text{Non-Circularity} = \frac{\textit{[The difference in shape between the artificial and the planetary objects]}}{\textit{[The total area of the planet]}}$$

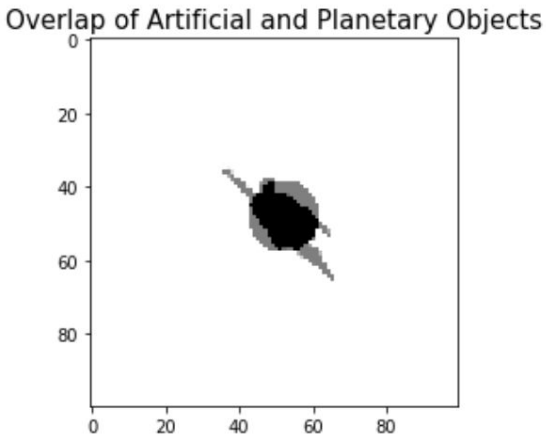

Figure 9: I calculate non-circularity of an artificial object by counting the number of gray pixels when I overlap the two objects and then dividing that number by the total area of the planet. In this case, the Superman object is 55% non-circular.

Using this measurement of non-circularity, we characterized many shapes and then measured their observability using the observability index outlined above.

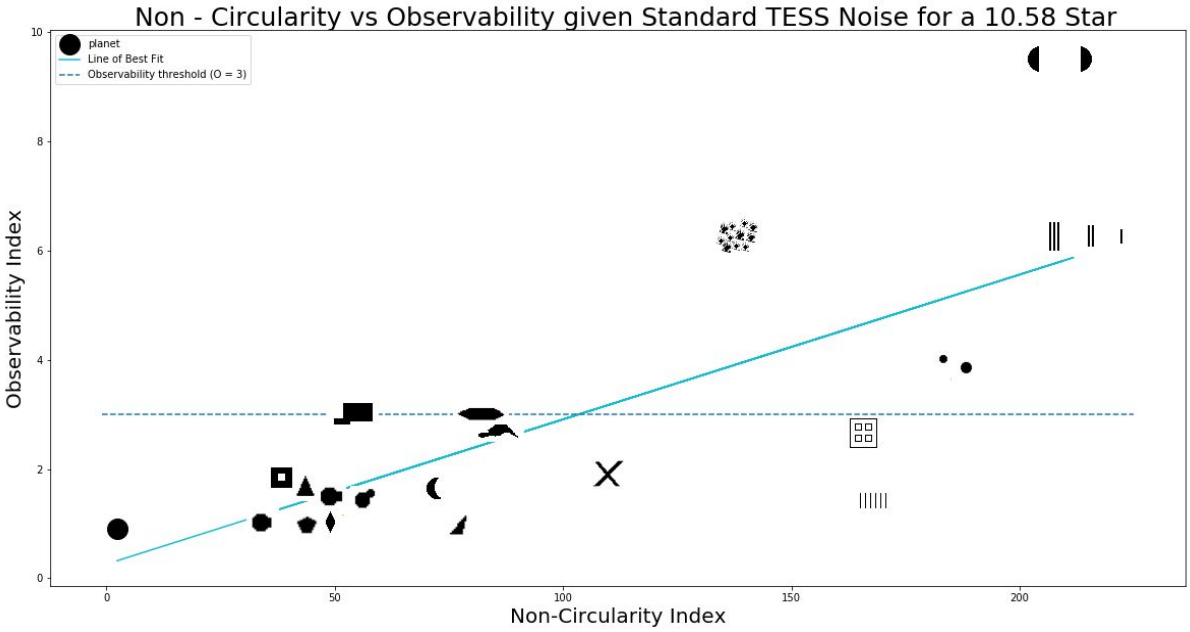

Figure 10: The observabilities (in front of a 10.58 magnitude star) of the different artificial and natural objects characterized by their non-circularity. The dotted line represents the observability threshold at which we are almost entirely certain an object is distinguishable from a planet. A few key objects include the planet, which plausibly, is indistinguishable from a planet while the two semi-circles shape is very distinguishable from a planet. Additionally, the two planets' shape is observable as something different than a planet.

Because the above plot only outlines the relationship between non-circularity and observability for a 10.58 magnitude star, we wanted to map the non-circularity index at which the line of best fit crosses the observability threshold for each magnitude. In the plot above, this is where the two blue lines cross.

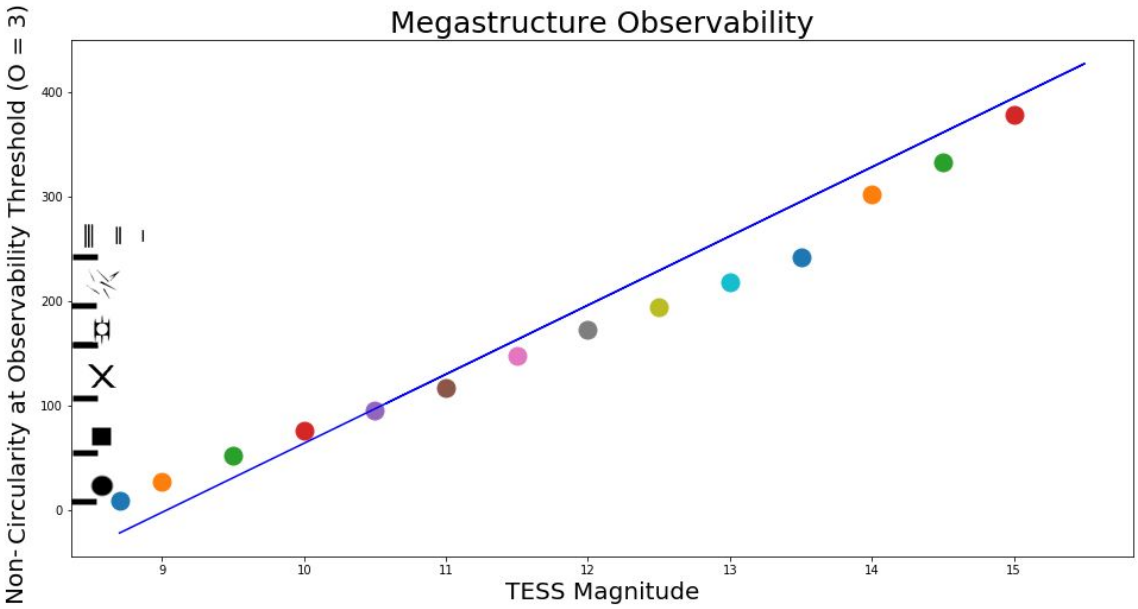

Figure 11: The non-circularity index at the observability threshold (O = 3) at different magnitudes within TESS' sweet spot (9th - 15th magnitude). The objects on the y axis demonstrate what each level of non-circularity looks like.

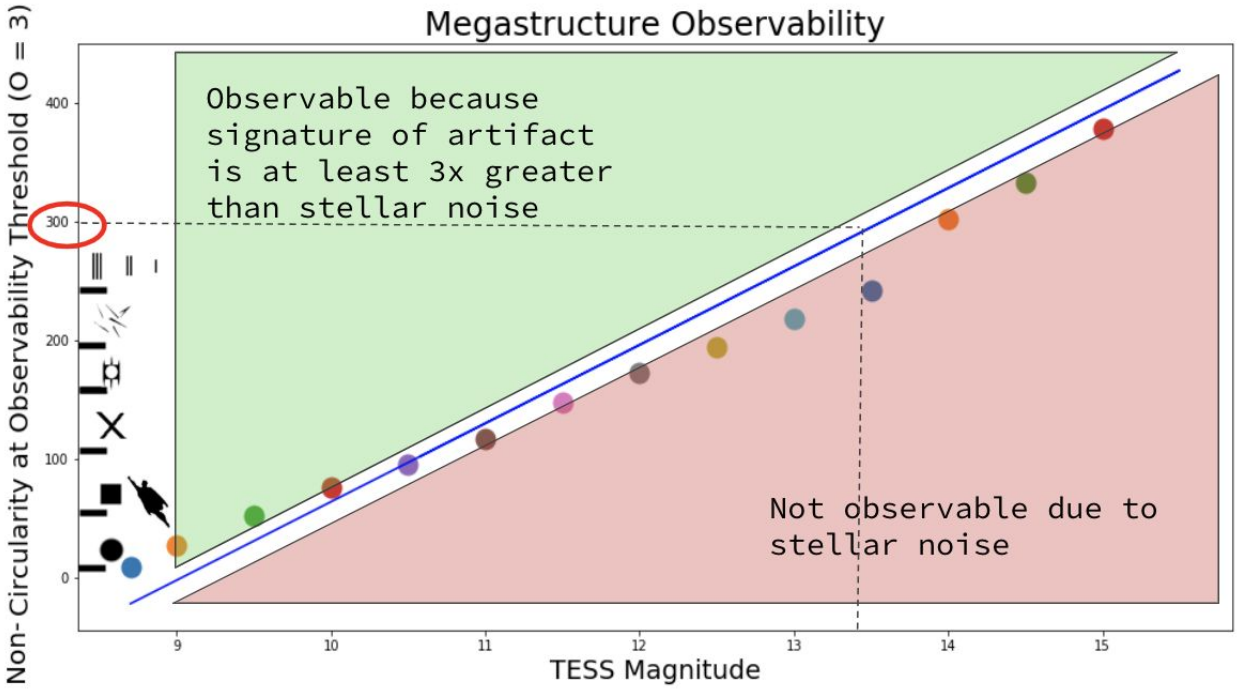

Figure 12: The non-circularity index at the observability threshold of O = 3. This plot includes the green and red sectors to distinguish between the range of magnitudes and their corresponding non-circularities at the observability threshold. Objects that fall in the green sector are observable because their signal within the residual in-transit RMS is at least three times greater than their noise within the residual out-of-transit RMS. Objects that fall in the red sector are not observable as something different than a planet because the stellar noise is too great to reveal the key characteristics of the light curve that allow an observer to differentiate between a planetary and a megastructure transit. The 300 non-circularity mark on the y axis is marked because

above this point, megastructures are 300% non-circular and through testing, they are indistinguishable from dust. Thus, a crude cut off of megastructure bearing stars could be deduced to be 13.5 magnitude where any stars dimmer than 13.5 magnitude would be considered incredibly poor or non-viable candidates for megastructure observation.

Goddard Data:

In late June of 2020, the Goddard Team generously gave Breakthrough Listen's Berkeley SETI Research Center access to 60 million light curves they calibrated in three forms (raw flux, PCA flux, and corrected flux). The data also includes quality flags generated by the Goddard Team as well as information about the sector, magnitude, RA and DEC, and TIC number of the object of interest. This dataset is made available through Google Cloud. For information on creating a google cloud account and accessing the Goddard Data, see this document: Guide to Creating a Virtual Instance with Google Cloud.

Because of the inability to distinguish between dust and megastructures at a non-circularity index of 300% or higher, a crude cut can be placed on megastructure bearing star candidates of 13.5 magnitude or brighter (see figure 12 for more information). Based on this threshold, there are 22,207,719 light curves within the Goddard data that are viable for megastructure observation simply using the photometric, single band data provided by TESS.

Conclusion and Future Work:

The three major take-aways that I learned from this summer are:

1. It is possible to model any artificial megastructure's transit light curve in front of its host star and calculate the observability of that artificial object.
2. Size, shape, and star magnitude all affect observability because they all affect transit shape (which, because we are only using the light curve as an indicator of a megastructure, transit shape is all we have to work with). Additionally, objects with a circularity of ~300 or greater are effectively indistinguishable from dust, meaning that stars with a magnitude of ~13.5 of dimmer are poor candidates for observing megastructures.
3. This work surrounding observability and non-circularity of ETI megastructures has implications that can be used to inform future megastructure system candidates.

The next steps that need to be taken to further inform this work on megastructure observability include parsing through the Goddard data. Giles and Walkowicz 2019 laid out a framework for searching through Kepler data using both machine learning techniques as well as a simpler statistical approach. These tools can be adapted to the Goddard dataset and hopefully be useful to determine key factors of possible megastructure candidates including strange periodicities, odd transit shapes, and general star dimming.

Using these relationships between non-circularity and observability within TESS light curves, we can more effectively create a statistical approach to search for observable artificial megastructures within TESS data. Our next step is to characterize other parameters that might differentiate artificial objects from natural ones and employ them alongside our knowledge of non-circularity and transit shape to search for artificial objects hidden in TESS data.

Key Links:

TechnoClimes Poster for their 2020 gathering
Final Presentation for BSRC Summer 2020
Github/BSRC_Summer_2020

References:

Sandford and Kipping 2018.
Arnold 2005.
Rappaport et al. 2019.
Wright et al. 2015.
Giles and Walkowicz 2019.

Contact information:
Piper Stacey
piper.f.stacey.23@dartmouth.edu